Study of stress evolution on lithium metal anodes via Fiber Bragg Grating (FBG) sensing technology

Experimental section

Materials

Lithium foil (450 μm thick) was purchased from Tianjin Zhongneng Lithium Industry. Copper wire (120 μm diameter) for the reference electrode was obtained from Anjieshun Co. Electrolyte solvents (EC, EMC, DMC, FEC) and the lithium salt ($LiPF_6$) were battery-grade and purchased from Suzhou Duodu Chemical Reagent Co. N-Methy l-2-pyrrolidinone (NMP) was supplied by Aladdin Reagent, and $Li_4Ti_5O_{12}$ (LTO) powder was purchased from Shenzhen Kejing. The fiber Bragg grating (FBG, Wuhan Ligong Guangxin) had a grating length of 5 mm, a cladding diameter of ~125 μm, a center wavelength of 1550 ± 0.3 nm, and a side-mode suppression ratio >15 dB. LTO electrodes were prepared by mixing LTO powder, Super P conductive carbon, and polyvinylidene fluoride (PVDF) binder in a weight ratio of 90:5:5 in NMP solvent. The slurry was coated onto aluminum foil, dried at 80 °C for 12 h, and then punched into discs with a diameter of 14 mm.

Cell Assembly and Testing

FBG-integrated cell: A custom-made polytetrafluoroethylene (PTFE) Swagelok-type cell with an internal diameter of 14 mm was used. It featured two side openings for inserting the FBG and the reference electrode. The cell was assembled by stacking the components in the following order: Li foil / FBG / polyethylene (PE) separator / lithiated-copper-wire reference electrode / glass fiber separator / LTO cathode. 150 μL of electrolyte was added. The assembled cell was compressed to 0.5 MPa using a custom clamping fixture equipped with springs to maintain constant pressure. After resting at 25 °C for 24 h, galvanostatic cycling with a fixed areal capacity was performed.

Li-Li symmetric cell: Standard 2032-type coin cells were assembled with Li discs (12 mm and 14 mm diameter on each side) in the configuration: Li / PE separator / glass fiber separator / PE separator / Li, with 65 μL of electrolyte.

Li-Cu cell: Standard 2032-type coin cells were assembled with a 14 mm Li disc and a 12 mm Cu foil in the configuration: Li / PE separator / glass fiber separator / PE separator / Cu foil, with 65 μL of electrolyte. Cells were crimp-sealed at 800 psi using a manual hydraulic crimper.

Chronoamperometry (CA) cell: Cells were assembled similarly to the Li-Li symmetric cells, but with a lithiated copper wire reference electrode placed between the PE and glass fiber separators to study the nucleation behavior of the 12 mm Li electrode.

All cell assembly was performed in an argon-filled glovebox (O_2 < 0.01 ppm, H_2O < 0.01 ppm). Electrochemical tests were conducted using a Neware battery test system (CT-4008) inside a temperature chamber set at 30 °C.

Electrochemical impedance spectroscopy (EIS): Measurements were performed using a two-electrode configuration on a CHI760F electrochemical workstation (CH Instruments) with an AC amplitude of 5 mV over a frequency range of 0.01 Hz to 1 MHz.

Chronoamperometry (CA): Measurements were performed using a three-electrode configuration on the CHI760F workstation. A potential step of 150 mV (absolute value) was applied, with a sampling interval of 0.001 s.

Material Characterization

Scanning electron microscopy (SEM): Surface and cross-sectional morphologies of Li electrodes were characterized using field-emission SEM (Hitachi SU8010) at an accelerating voltage of 5 kv.

Raman spectroscopy: Raman spectra of the FBG before and after cell operation were collected using a Renishaw inVia confocal Raman microscope. A 633 nm He-Ne laser was focused through a 50× long-working-distance objective (Leica). Spectra were

acquired with 120 s integration time, 10% laser power, and a resolution of ~1.0 cm^{-1}.

Optical microscopy: Post-cycling Li electrodes retrieved from disassembled coin cells were placed in a sealed quartz holder for observation under an optical microscope.

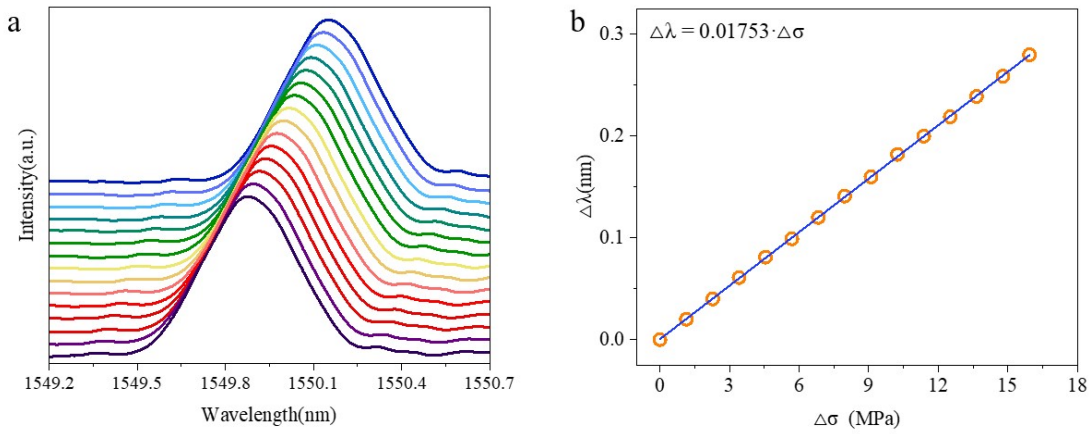

Fig. S1. Thewavelength-stress calibration experiment of FBG. (a) 2D stack-view of the reflected spectra given by the FBG sensor after hanging the weights. (b) The fitted response curve of wavelength towards vertical stress. The slope of the response curve is calculated to be 17.53 pm MPa^{-1}.

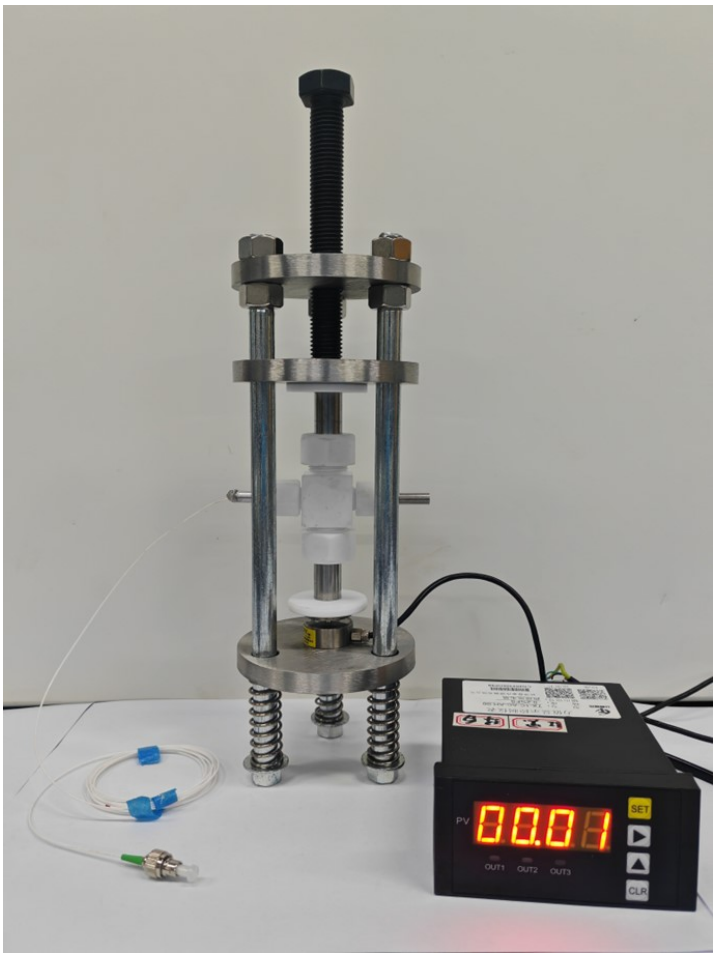

Fig. S2. The complete battery device used in this research.

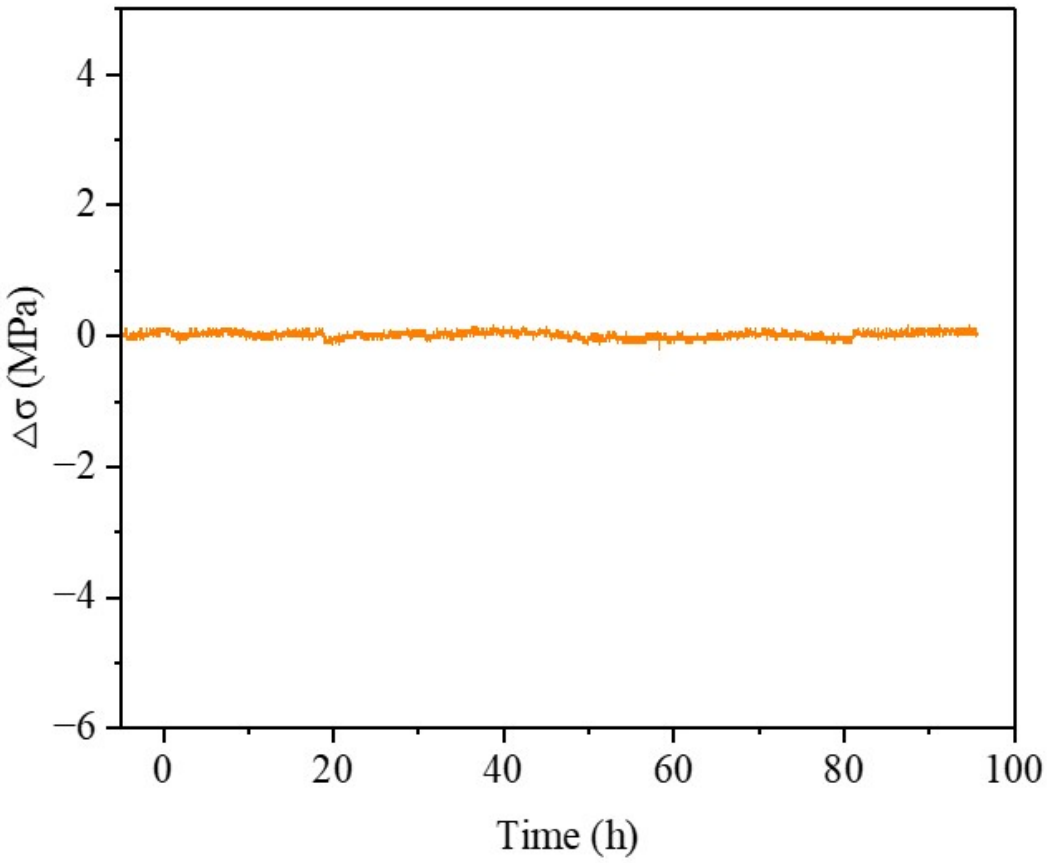

Fig. S3. Stress signal of temperature and air pressure monitoring FBG.

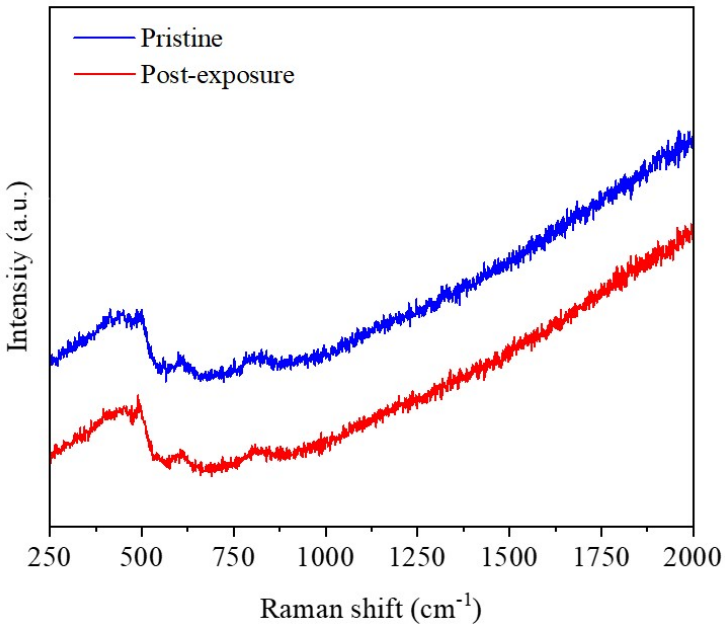

Fig. S4. Raman spectra of the same FBG at different stage.The blue curve represents the initial state.The red curve represents after 200 h of cycling at 1 mA cm^{-2}, 1 mAh cm^{-2} in EL1.

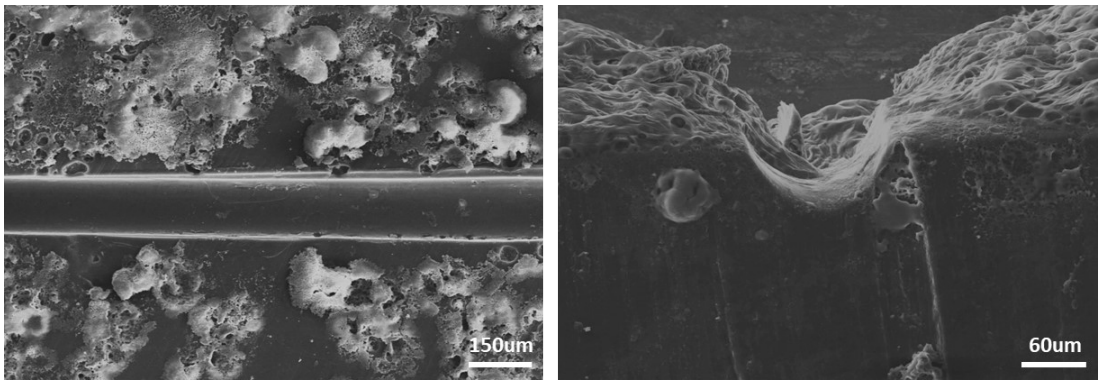

Fig. S5. Top-View and cross-sectional SEM images after the first plating at 0.2 mA cm^{-2}, 1 mAh cm^{-2} at the location of removing the FBG in EL1.

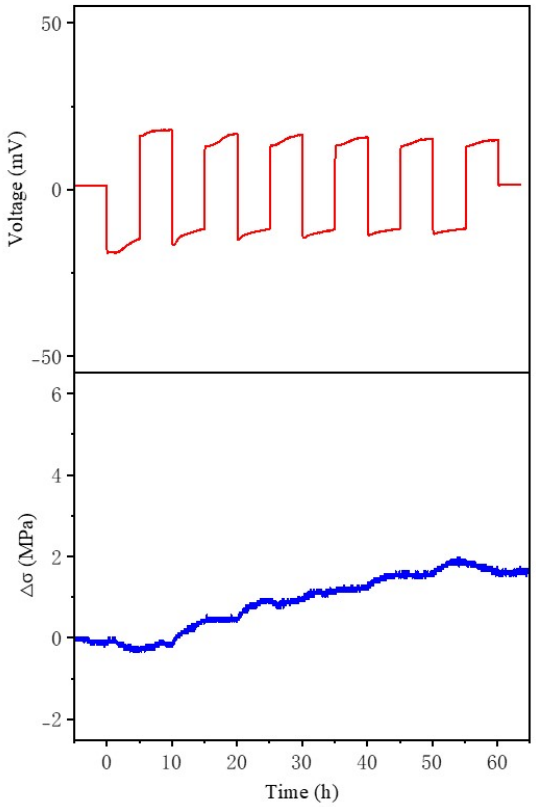

Fig. S6. Time-resolved voltage (top) and stress evolution of FBG (bottom) placed on the bottom of lithium metal electrode in EL1 electrolyte at 0.2 mA cm^{-2}, 1 mAh cm^{-2}.

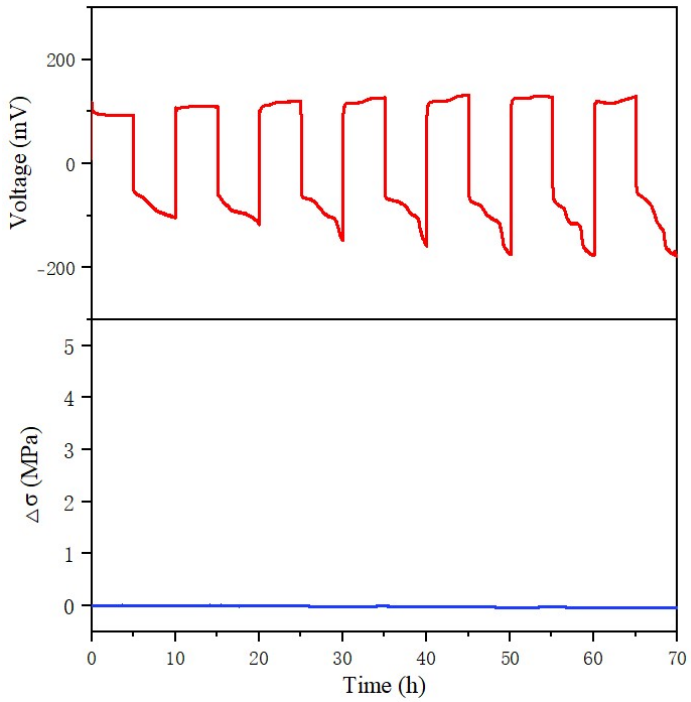

Fig. S7. Time-resolved voltage (top) and external cycling pressure (bottom) of the cell using EL1 electrolyte at 0.2 mA cm^{-2}, 1 mAh cm^{-2}.

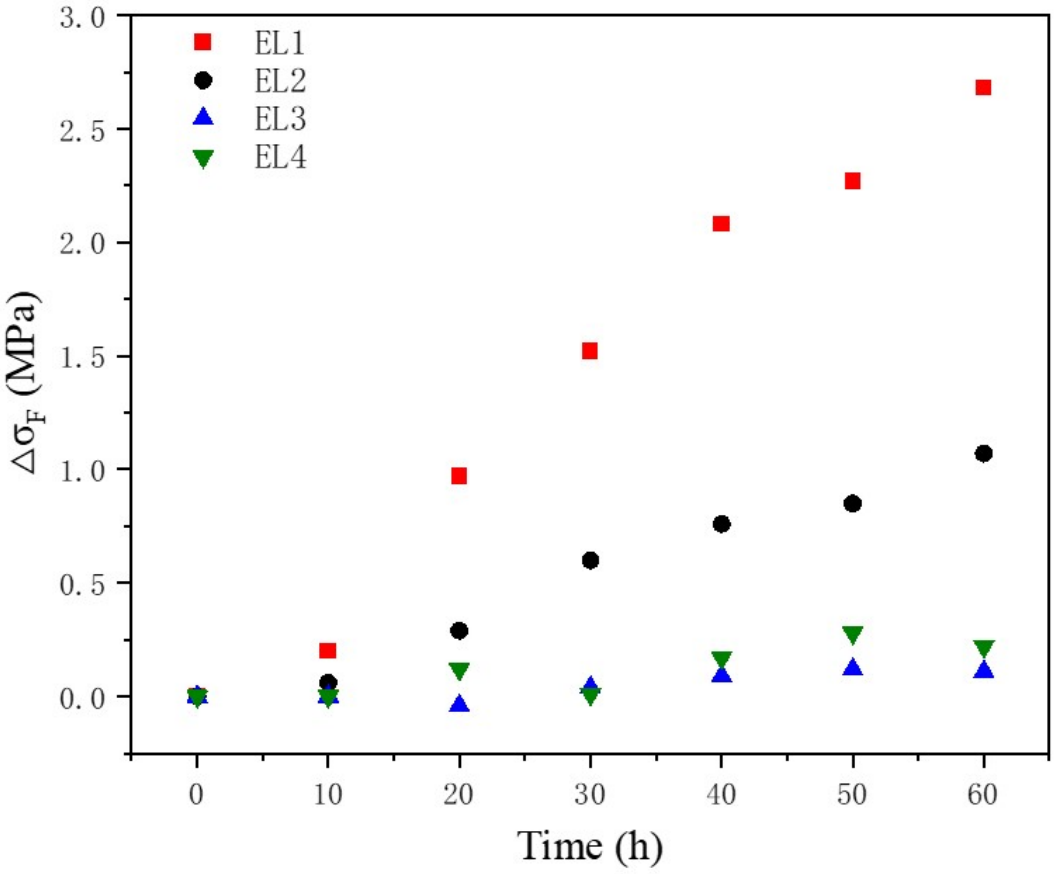

Fig. S8. The evolution of baeline stress ($\Delta\sigma_F$) at 0.2 mA cm^{-2}, 1 mAh cm^{-2} in different electrolyte.

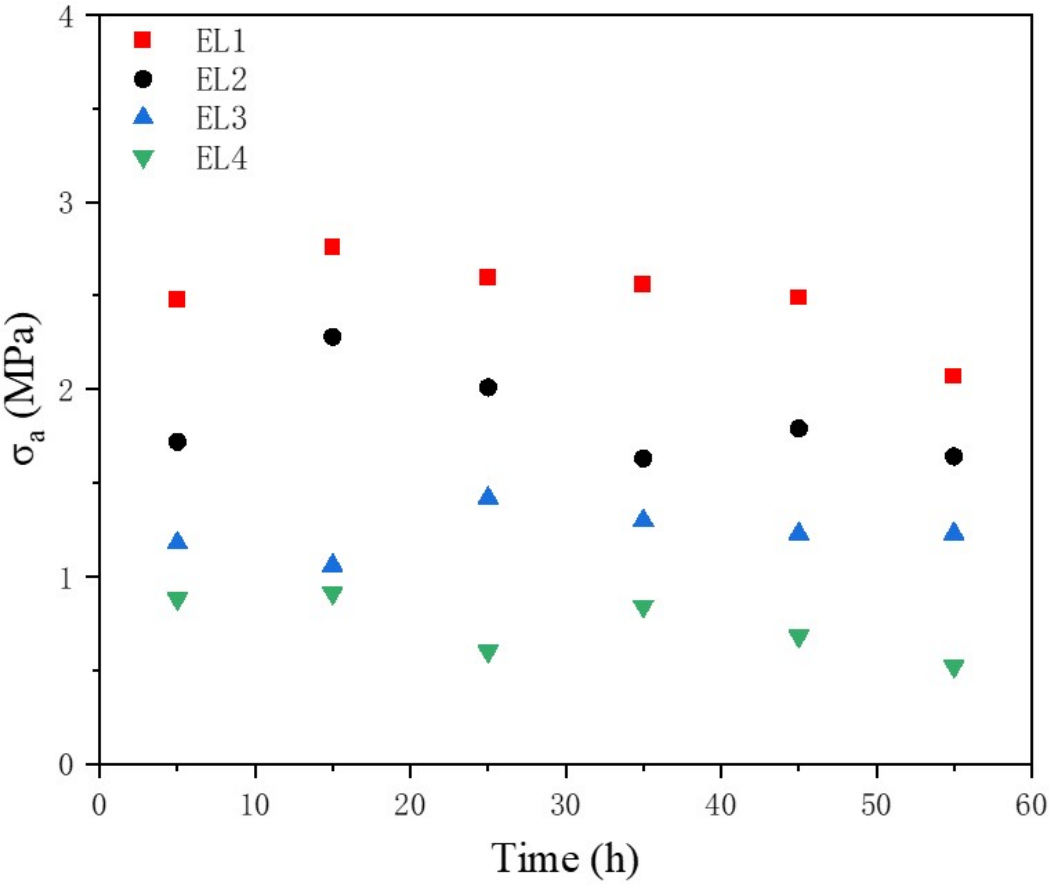

Fig. S9. The evolution of stress amplitude (σ_a) at 0.2 mA cm^{-2}, 1 mAh cm^{-2} in different electrolyte.

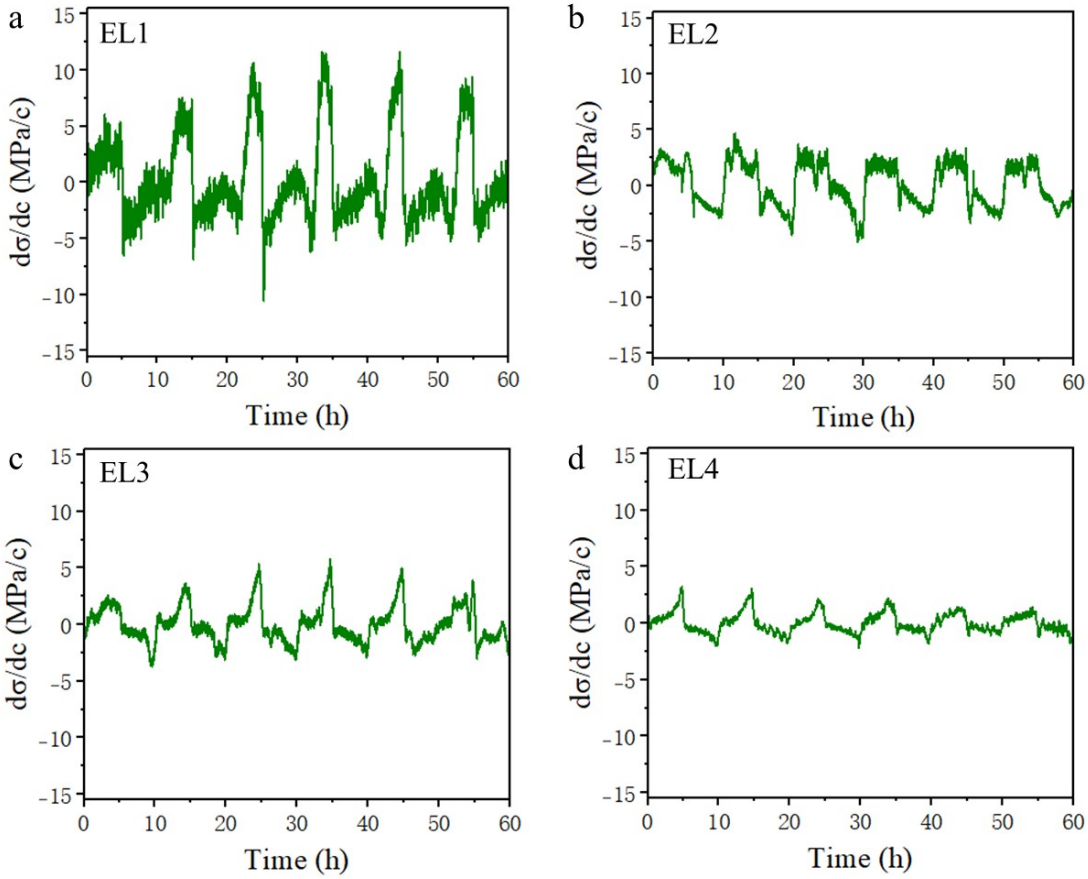

Fig. S10. The time-"dσ/dc" curves about stress evolution of FBG in different electrolyte at 0.2 mA cm^{-2} and 1 mAh cm^{-2}.

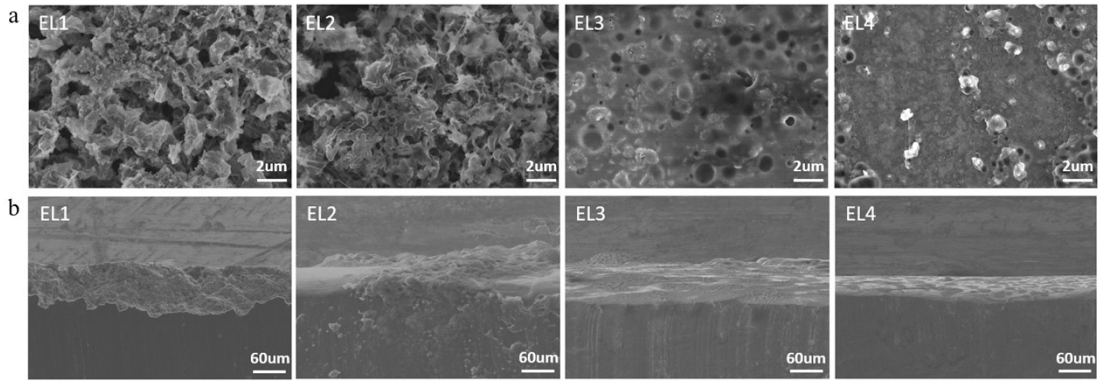

Fig. S11. Top-View (a) and cross-sectional (b) SEM images of the Lithium metal electrode after the stripping in sixth cycle at 0.2 mA cm^{-2}, 1 mAh cm^{-2} in different electrolytes.

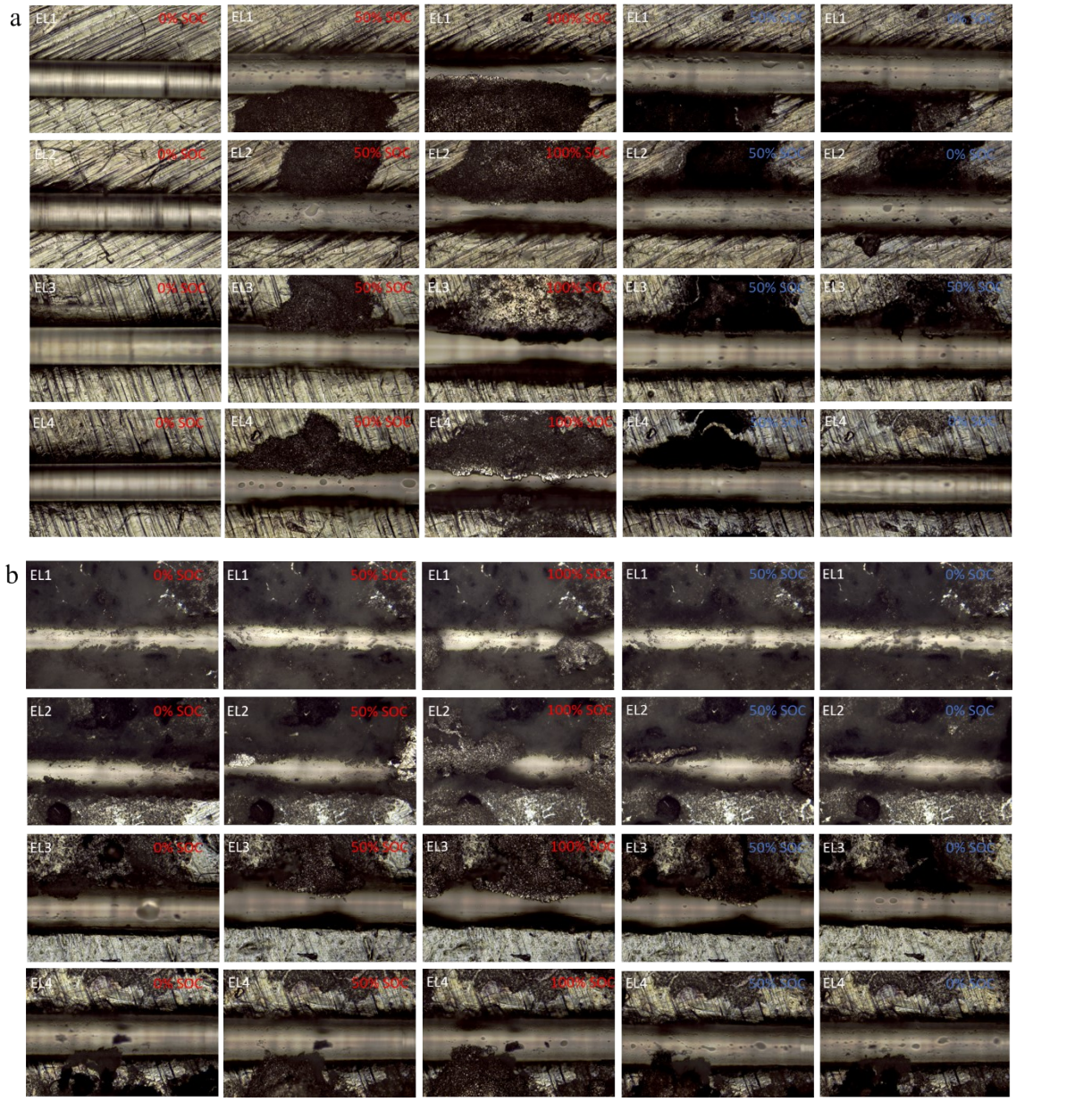

Fig. S12. Optical microscope images of FBG placed on the surface of lithium metal electrode at the same location during (a) the first and (b) sixth cycles of lithium deposition at different SOC stages at 0.2 mA cm^{-2} and 1 mAh cm^{-2}.

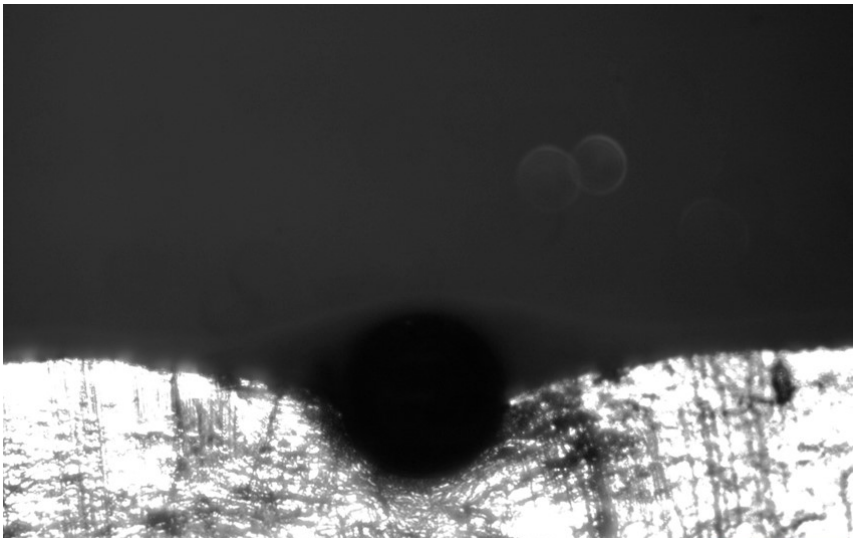

Fig. S13. Optical microscope images of FBG placed on the surface of lithium metal electrode in a complete battery

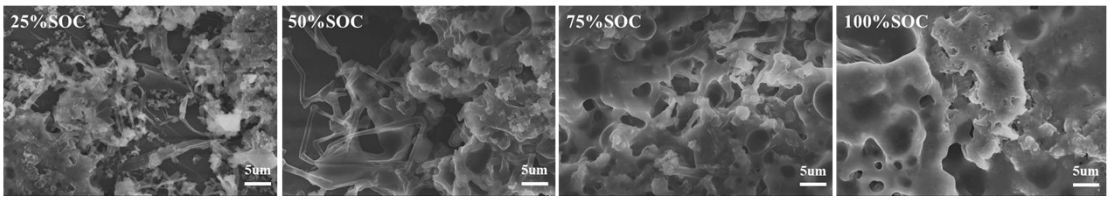

Fig. S14. Top-View SEM images of the Lithium metal electrode at different SOC condition of deposition during second cycle at 0.2 mA cm^{-2}, 1 mAh cm^{-2} in EL1.

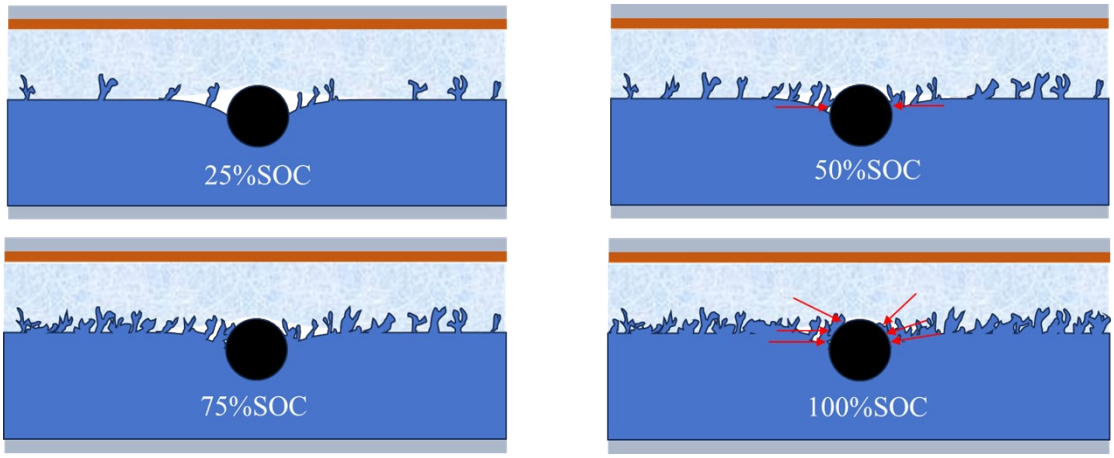

Fig. S15. The stress simulation of FBG on the lithium metal electrodes at different SOC condition of deposition at 0.2 mA cm^{-2}, 1 mAh cm^{-2} in EL1.

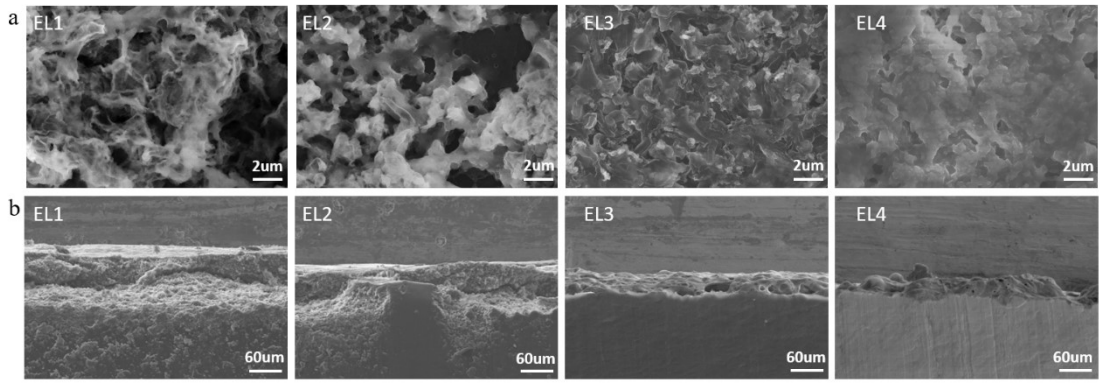

Fig. S16. Top-View (a) and cross-sectional (b) SEM images of the Lithium metal electrode after the stripping in fiftieth cycle at 1 mA cm^{-2}, 1 mAh cm^{-2} in different electrolytes.

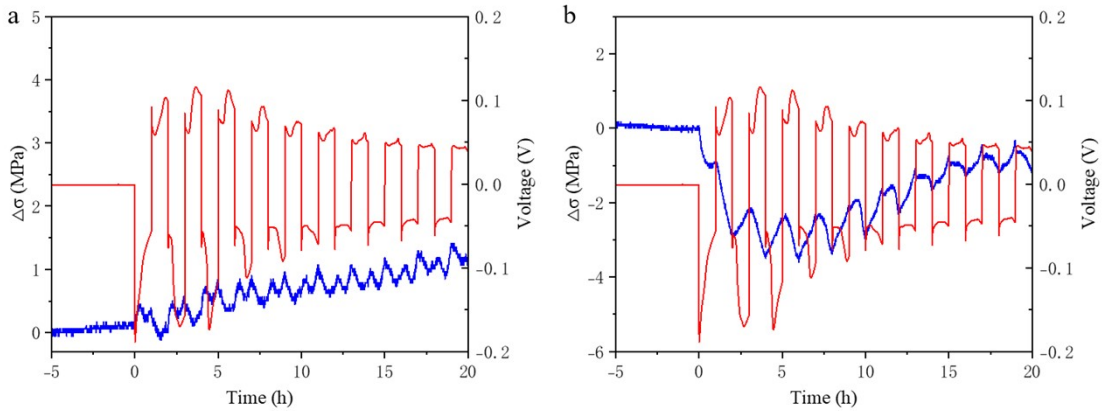

Fig. S17. The stress evalution of FBG placed at different location (blue curves) with corresponding time-voltage curves (red curves):(a) on the top of the PE diaphragm,(b) at the bottom of the PE diaphragm.

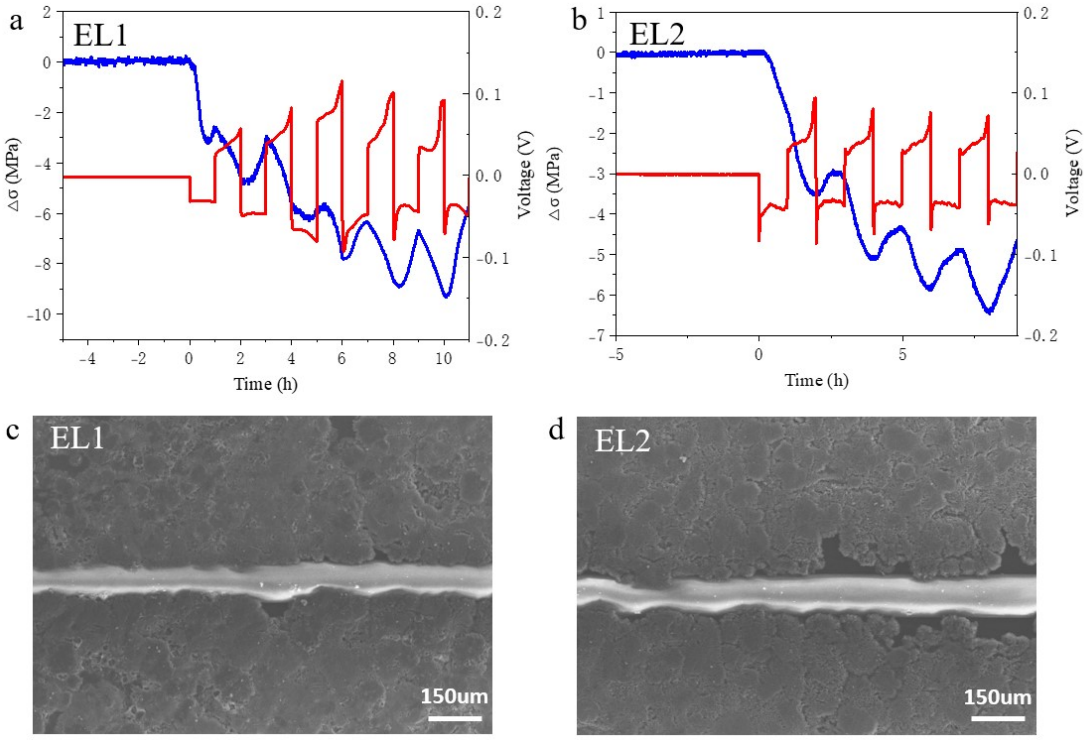

Fig. S18. (a,b) The stress evalution of FBG (blue curves) with corresponding time-voltage curves (red curves) at the turning point of $\Delta\sigma_F$ after lithium plating with corresponding (c,d) top view of SEM images.

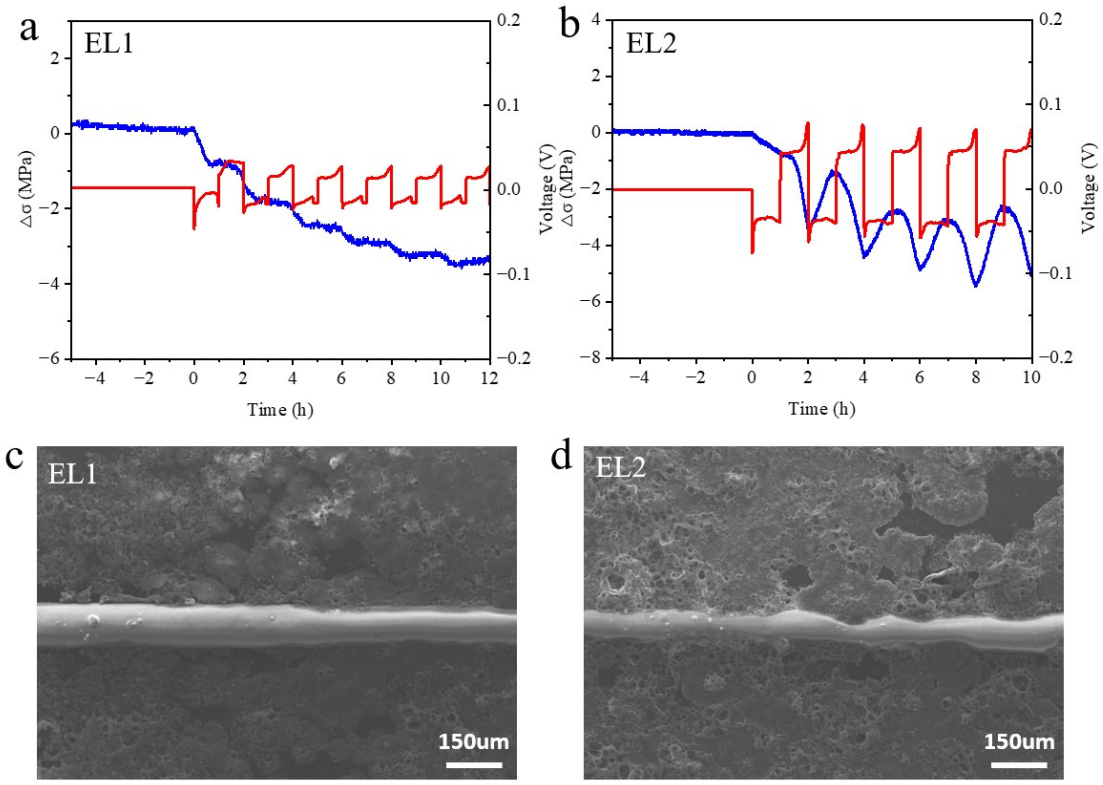

Fig. S19. (a,b) The stress evalution of FBG (blue curves) with corresponding time-voltage curves (red curves) at the turning point of $\triangle\sigma_F$ after lithium stripping with corresponding (c,d) top view of SEM images.

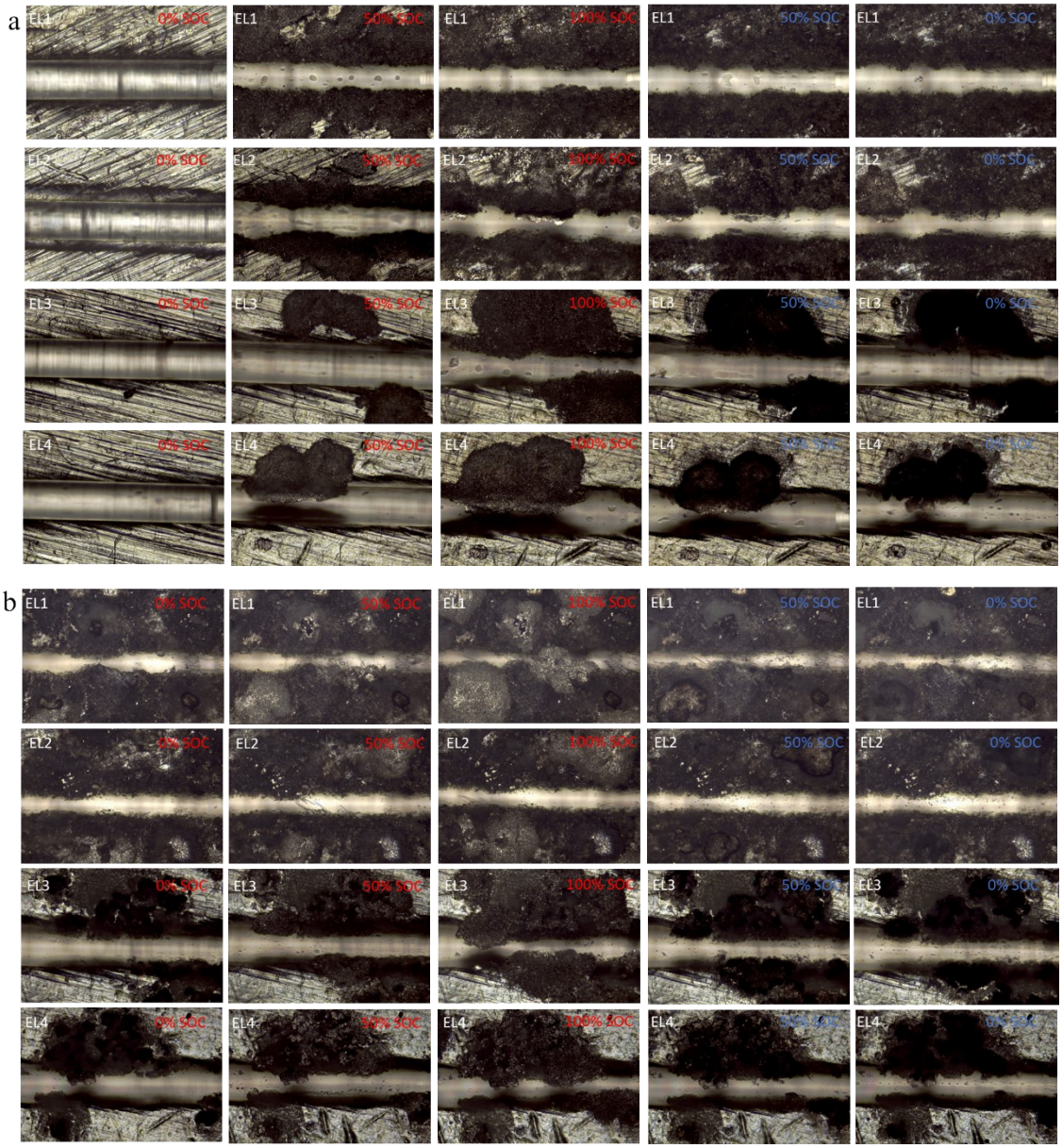

Fig. S20. Optical microscope images of FBG placed on the surface of lithium metal electrode at the same location during (a) the first and (b) sixth cycles of lithium deposition at different SOC stages at 1 mA cm^{-2} and 1 mAh cm^{-2}.